Singular perturbation based neuro-H∞ control scheme for a manipulator with flexible links and joints

B. Subudhi† and A. S. Morris‡

SUMMARY

A novel composite control scheme for a manipulator with flexible links and joints is presented that uses the singular perturbation technique (SPT) to divide the manipulator dynamics into reduced order slow and fast subsystems. A neural network controller is then applied for the slow subsystem and a state-feedback H_∞ controller for the fast subsystem. Results are presented that demonstrate improved performance over an alternative SPT-based controller that uses inverse dynamics and LQR controllers.

KEYWORDS: Neuro-H_∞ control; Singular perturbation; Flexible links.

I. INTRODUCTION

During the last three decades, there has been great interest within the research community in the design and control of robot manipulators with flexible links and joints since these have a number of advantages.[1] Controlling flexible-link manipulators is difficult because discretization of the partial differential equations describing the coupled rigid and flexible motions gives rise to dynamical systems of high order. In addition, the system is underactuated because the number of available control inputs is less than the number of degrees of freedom, i.e. all modes of flexure in a link and its desired trajectory have to be controlled simultaneously by adjusting a single actuating torque. This difficulty is accentuated in the case where both the links and joints are flexible since the actuating torque for each link then has to control the flexure of both the link and its corresponding joint.

The singular perturbation technique (SPT) is useful in such systems since it allows the full-order complex dynamics to be divided into simpler subsystems consisting of the reduced order slow dynamics and the fast dynamics. Separate sub-controllers can then be designed for the slow and fast subsystems and combined into a composite controller for the whole system.

SPT-based controllers have previously been applied to manipulators where either link or joint flexibility is considered.[1,2] However, SPT had not been applied for

† Dept. of Electrical Engineering, Indira Gandhi Institute of Technology, Sarang-759146, Orissa, (India).
‡ Dept. of Automatic Control & Systems Engineering, Mappin Street, Sheffield S1 3JD, University of Sheffield (UK). Corresponding author. E-mail: acse@sheffield.ac.uk

controllers that take account of flexibility in both links and joints together until the recently published paper by the authors,[3] in which the slow subsystem comprises the non-flexible motion of the links and joints and the fast subsystem comprises the flexible modes of the links and joints. In this implementation of SPT, an integral manifold approach was used to derive corrected slow and fast models. Then, an inverse dynamics (computed torque) method was used to control the slow dynamics and a linear quadratic regulator (LQR) algorithm was applied for the linearised fast dynamics, in a similar fashion to earlier work.[2,4]

Whilst the integral manifold approach is useful for obtaining corrected slow and fast subsystems, solution of the manifold equations becomes very complicated when higher order perturbation terms are considered. Computational limitations mean that it is necessary to approximate the manifold expansion, which, together with unmodelled high-frequency modes, leads to model uncertainty that is reflected into the slow dynamics. Unfortunately, the inverse dynamics technique requires a perfect model so that the gains of the controller can be chosen to achieve a critically damped system response,[2,4] and this perfect model condition is clearly not met. Likewise, the LQR technique becomes unsatisfactory when there is uncertainty in the fast subsystem. Thus, faced with uncertainty in both slow and fast sub-systems, better controllers that take proper account of this uncertainty are needed, as developed in this paper.

II. MODELLING USING THE SINGULAR PERTURBATION TECHNIQUE

Figure 1 shows the structure of a manipulator with n-flexible serial links and n-flexible actuated joints, with an inertial payload of mass m_p and inertia I_p. Each flexible joint is modelled as a linear torsional spring that connects the rotor of the joint actuator to the link. α_i, θ_i are the ith rotor and link angular positions. I_{ri} is the ith rotor inertia, $u_i(t)$ is the input torque, N_i is the gear ratio for the ith rotor and k_{si} is the spring constant of the ith flexible joint (FJ)$_i$.

Applying the Euler-Lagrange principle and assumed modes method, the dynamic equations are:[3]

$$\mathbf{J}\ddot{\alpha} - \mathbf{K_s}(\theta - \alpha) = u \tag{1}$$

$$\mathbf{M}(\theta, q)\begin{Bmatrix}\ddot{\theta}\\\ddot{q}\end{Bmatrix} + \begin{Bmatrix}f_1(\theta, \dot{\theta})\\f_2(\theta, \dot{\theta})\end{Bmatrix} + \begin{Bmatrix}g_1(\theta, \dot{\theta}, q, \dot{q})\\g_2(\theta, \dot{\theta}, q, \dot{q})\end{Bmatrix}$$
$$+ \begin{Bmatrix}0\\\mathbf{D}\dot{q}\end{Bmatrix} + \begin{Bmatrix}\mathbf{K_s}(\theta - \alpha)\\\mathbf{K_w}q\end{Bmatrix} = \begin{Bmatrix}0\\0\end{Bmatrix} \tag{2}$$
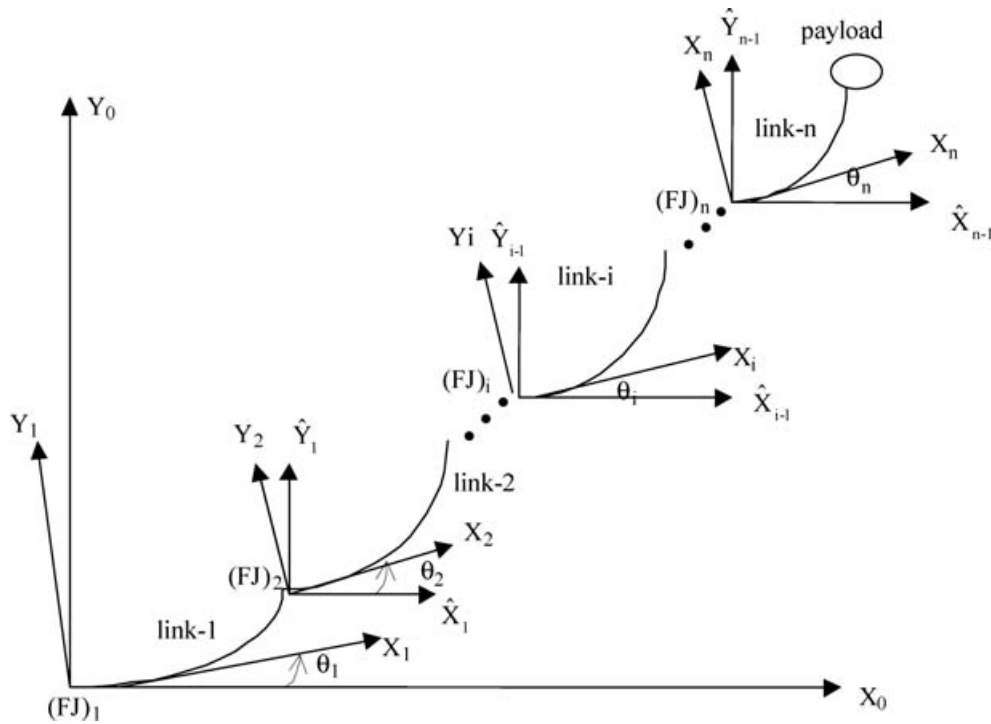
Fig. 1. Schematic diagram of the manipulator.

and the deflection of the ith link at a spatial point η_i along the link is:

$$v_i(\eta_i, t) = \sum_{j=1}^{m_i} q_{ij}(t)\phi_{ij}(\eta_i) \quad (3)$$

where:

$q_{ij}(t), \phi_{ij}(\eta_i) = j$th generalized modal-coordinate and mode shape function respectively;
m_i = number of modes for ith link;
$\mathbf{M} \in \Re^{(n+m)\times(n+m)}$ = symmetric positive definite mass matrix;
m = total number of flexible modes considered, i.e. $m = \sum_{i=1}^{n} m_i$;
$\mathbf{J} \in \Re^{n\times n}$ = rotor inertia matrix;
$\mathbf{K}_w \in \Re^{m\times m}$ = stiffness matrix related to link flexure;
$\mathbf{K}_s \in \Re^{n\times n}$ = stiffness matrix related to joint flexure;
$\mathbf{D} \in \Re^{m\times m}$ = structural damping matrix of the links;
$\boldsymbol{\theta} \in \Re^n$ = vector of link angular positions;
$\boldsymbol{\alpha} \in \Re^n$ = vector of rotor angular positions;
$\boldsymbol{q} \in \Re^m$ = vector of generalized co-ordinates;
$\boldsymbol{f}_1 \in \Re^n, \boldsymbol{f}_2 \in \Re^m$ = coriolis, centrifugal force vectors;
$\boldsymbol{g}_1 \in \Re^n, \boldsymbol{g}_2 \in \Re^m$ = vectors containing product terms between the link angular positions and the generalized flexible co-ordinates and their derivatives.

A singular perturbation model can be obtained as follows: Since the mass matrix $\mathbf{M}(\cdot)$ is positive definite, its inverse $\mathbf{H}(\cdot)$ exists. The rigid and flexible acceleration vectors $\ddot{\boldsymbol{\theta}}$ and $\ddot{\boldsymbol{q}}$ can be obtained in terms of $\mathbf{H}(\cdot)$ from (1):

$$\ddot{\boldsymbol{\theta}} = -\mathbf{H}_{11}(\theta, q)[f_1(\theta, \dot{\theta}) + g_1(\theta, \dot{\theta}, q, \dot{q}) - \mathbf{K}_s\delta]$$
$$- \mathbf{H}_{12}(\theta, q)[f_2(\theta, \dot{\theta}) + g_2(\theta, \dot{\theta}, q, \dot{q})$$
$$+ \mathbf{K}_w q + D\dot{q}] \quad (4)$$

$$\ddot{\boldsymbol{q}} = -\mathbf{H}_{21}(\theta, q)[f_1(\theta, \dot{\theta}) + g_1(\theta, \dot{\theta}, q, \dot{q}) - \mathbf{K}_s\delta]$$
$$- \mathbf{H}_{22}(\theta, q)[f_2(\theta, \dot{\theta}) + g_2(\theta, \dot{\theta}, q, \dot{q})$$
$$+ \mathbf{K}_w q + D\dot{q}] \quad (5)$$

Subtracting $\mathbf{J}\ddot{\boldsymbol{\theta}}$ from both sides of (1), multiplying both sides by $\mathbf{J}^{-1}$ and setting $\delta = (\alpha - \theta)$:

$$\ddot{\boldsymbol{\delta}} = \ddot{\boldsymbol{\alpha}} - \ddot{\boldsymbol{\theta}} = -\mathbf{J}^{-1}\mathbf{K}_s\delta + \mathbf{J}^{-1}\boldsymbol{u} - \ddot{\boldsymbol{\theta}} \quad (6)$$

Let k_c be a common scale factor extracted from the link and joint stiffness constants:

$$k_c = \min(k_{11}, k_{12}, \ldots, k_{1m_1}, \ldots, k_{n1}, k_{n2},$$
$$\ldots, k_{nm_n}, k_{s1}, \ldots k_{sn}) \quad (7)$$

Then μ can be used as the perturbation parameter to scale $\mathbf{K}_s$ and $\mathbf{K}_w^1$, where $\mu = 1/k_c$:

$$\tilde{\mathbf{K}}_s = \mu\mathbf{K}_s \quad \text{and} \quad \tilde{\mathbf{K}}_w = \mu\mathbf{K}_w \quad (8)$$

Defining $\boldsymbol{q} = \mu\xi_q, \delta = \mu\xi_\delta$ and substituting these into (4–6):

$$\ddot{\boldsymbol{\theta}} = -\mathbf{H}_{11}(\theta, \mu\xi_q)\{f_1(\theta, \dot{\theta}) + g_1(\theta, \dot{\theta}, q, \dot{q}) - \mathbf{K}_s\mu\xi_\delta\}$$
$$- \mathbf{H}_{12}(\theta, \mu\xi_q)\{f_2(\theta, \dot{\theta}) + g_2(\theta, \dot{\theta}, \mu\xi_q, \mu\dot{\xi}_q)$$
$$+ \mathbf{K}_w\mu\xi_q + D\mu\dot{\xi}_q\} \quad (9)$$

$$\mu\ddot{\xi}_q = -\mathbf{H}_{21}(\theta, \mu\xi_q)\{f_1(\theta, \dot{\theta}) + g_1(\theta, \dot{\theta}) - \mathbf{K}_s\mu\xi_\delta\}$$
$$- \mathbf{H}_{22}(\theta, \mu\xi_q) f_2(\theta, \dot{\theta}) + g_2(\theta, \dot{\theta}, \mu\xi_q, \mu\dot{\xi}_q)$$
$$+ \mathbf{K}_w\mu\xi_q + D\mu\dot{\xi}_q\} \quad (10)$$

$$\mu\ddot{\xi}_\delta = -\mathbf{J}^{-1}\tilde{\mathbf{K}}_s\xi_\delta + \mathbf{J}^{-1}\boldsymbol{u} - \ddot{\boldsymbol{\theta}} \quad (11)$$

Substituting $\ddot{\boldsymbol{\theta}}$ from (9), Eq. (11) can be rewritten as

$$\mu\ddot{\boldsymbol{\xi}}_\delta = -\mathbf{J}^{-1}\tilde{\mathbf{K}}_s\,\boldsymbol{\xi}_\delta + \mathbf{J}^{-1}\boldsymbol{u} + \mathbf{H_{11}}(\theta, \mu\xi_q)\{\boldsymbol{f_1}(\theta, \dot{\theta})$$
$$+ \boldsymbol{g_1}(\theta, \dot{\theta}, \mu\xi_q, \mu\dot{\xi}_q) - \mathbf{K_s}\mu\xi_\delta\}$$
$$+ \mathbf{H_{12}}(\theta, \mu\xi_q)\{\boldsymbol{g_2}(\theta, \dot{\theta}, \mu\xi_q, \mu\dot{\xi}_q) + \boldsymbol{f_2}(\theta, \dot{\theta})$$
$$+ \mathbf{K_w}\mu\xi_q + \mathbf{D}\mu\dot{\boldsymbol{\xi}}_q\} \tag{12}$$

The slow system can be found[1] by setting μ to zero in (10, 11):

$$\bar{\xi}_q = \tilde{\mathbf{K}}_w^{-1}\mathbf{H_{22}^{-1}}(\bar{\theta}, \mathbf{0})[-\mathbf{H_{21}}(\bar{\theta}, \mathbf{0})\boldsymbol{f_1}(\bar{\theta}, \dot{\bar{\theta}})$$
$$- \mathbf{H_{22}}(\bar{\theta}, \mathbf{0})\boldsymbol{f_2}(\bar{\theta}, \dot{\bar{\theta}}) + \mathbf{H_{21}}(\bar{\theta}, \mathbf{0})\tilde{\mathbf{K}}_s\bar{\xi}_\delta] \tag{13}$$
$$\bar{\xi}_\delta = \tilde{\mathbf{K}}_s^{-1}(\bar{\boldsymbol{u}} - \mathbf{J}\ddot{\bar{\theta}}) \tag{14}$$

Substituting from (13) and (14) in (9) and dropping the arguments from the **H** sub-matrices for clarity gives:[1]

$$\ddot{\bar{\theta}} = (-\mathbf{H_{11}} + \mathbf{H_{12}}\mathbf{H_{22}^{-1}}\mathbf{H_{21}})\boldsymbol{f_1}(\bar{\theta}, \dot{\bar{\theta}})$$
$$+ (\mathbf{H_{11}} - \mathbf{H_{12}}\mathbf{H_{22}^{-1}}\mathbf{H_{21}})(\bar{\boldsymbol{u}} - \mathbf{J}\ddot{\bar{\theta}}) \tag{15}$$

This represents the slow subsystem of the singularly perturbed model of the manipulator and can be written as:

$$\ddot{\bar{\theta}} = (\mathbf{M_{11}} + \mathbf{J})^{-1} \times \{-\boldsymbol{f_1}(\bar{\theta}, \ddot{\bar{\theta}}) + \bar{\boldsymbol{u}}\} \tag{16}$$

since $(\mathbf{H_{11}} - \mathbf{H_{12}}\mathbf{H_{22}^{-1}}\mathbf{H_{21}}) = \mathbf{H_{11}} = \mathbf{M_{11}^{-1}}$.

Let system state variables be defined as:

$$\boldsymbol{x}_1 = \boldsymbol{\theta}, \quad \boldsymbol{x}_2 = \dot{\boldsymbol{\theta}}, \quad \boldsymbol{y}_1 = \boldsymbol{\xi}_q, \quad \boldsymbol{y}_2 = \boldsymbol{\varepsilon}\,\dot{\boldsymbol{\xi}}_q, \quad \boldsymbol{y}_3 = \boldsymbol{\xi}_\delta,$$
$$\text{and } y_4 = \varepsilon\dot{\xi}_\delta, \quad \text{where } \varepsilon = \sqrt{\mu} \tag{17}$$

Now, substituting these state variables into (9–11) gives the singular perturbation model in state-space form:

$$\left.\begin{array}{l}\dot{x}_1 = x_2 \\ \dot{x}_2 = -\mathbf{H_{11}}(\boldsymbol{x}_1, \varepsilon^2\boldsymbol{y}_1)[\boldsymbol{f_1}(\boldsymbol{x}_1, \boldsymbol{x}_2) + \boldsymbol{g_1}(\boldsymbol{x}_1, \boldsymbol{x}_2, \varepsilon^2\,\boldsymbol{y}_1, \varepsilon\,\boldsymbol{y}_2) - \tilde{\mathbf{K}}_s\boldsymbol{y}_3] \\ \quad - \mathbf{H_{12}}(\boldsymbol{x}_1, \varepsilon^2\boldsymbol{y}_1)[\boldsymbol{f_2}(\boldsymbol{x}_1, \boldsymbol{x}_2) + \boldsymbol{g_2}(\boldsymbol{x}_1, \boldsymbol{x}_2, \varepsilon^2\,\boldsymbol{y}_1, \varepsilon\,\boldsymbol{y}_2) + \tilde{\mathbf{K}}_w\boldsymbol{y}_1]\end{array}\right\} \tag{18}$$

$$\left.\begin{array}{l}\varepsilon\,\dot{\boldsymbol{y}}_1 = \boldsymbol{y}_2 \\ \varepsilon\,\dot{\boldsymbol{y}}_2 = -\mathbf{H_{21}}(\boldsymbol{x}_1, \varepsilon^2\boldsymbol{y}_1, \varepsilon^2\boldsymbol{y}_1)[\boldsymbol{f_1}(\boldsymbol{x}_1, \boldsymbol{x}_2) \\ \quad + \boldsymbol{g_1}(\boldsymbol{x}_1, \boldsymbol{x}_2, \varepsilon^2\boldsymbol{y}_1, \varepsilon\boldsymbol{y}_2) - \tilde{\mathbf{K}}_s\boldsymbol{y}_3] \\ \quad - \mathbf{H_{22}}(\boldsymbol{x}_1, \varepsilon^2\boldsymbol{y}_1)[\boldsymbol{f_2}(\boldsymbol{x}_1, \boldsymbol{x}_2) \\ \quad + \boldsymbol{g_2}(\boldsymbol{x}_1, \boldsymbol{x}_2, \varepsilon^2\boldsymbol{y}_1, \varepsilon\boldsymbol{y}_2) + \tilde{\mathbf{K}}_w\boldsymbol{y}_1] \\ \varepsilon\,\dot{\boldsymbol{y}}_3 = \boldsymbol{y}_4 \\ \varepsilon\,\dot{\boldsymbol{y}}_4 = -\{\mathbf{H_{11}}(\boldsymbol{x}_1, \varepsilon^2\,\boldsymbol{y}_1) + \mathbf{J}^{-1}\}[-\tilde{\mathbf{K}}_s\boldsymbol{y}_3 \\ \quad + \boldsymbol{f_1}(\boldsymbol{x}_1, \boldsymbol{x}_2) + \boldsymbol{g_1}(\boldsymbol{x}_1, \boldsymbol{x}_2, \varepsilon^2\,\boldsymbol{y}_1, \varepsilon\boldsymbol{y}_2)] \\ \quad - \mathbf{H_{12}}(\boldsymbol{x}_1, \varepsilon^2\boldsymbol{y}_1)[\boldsymbol{f_2}(\boldsymbol{x}_1, \boldsymbol{x}_2) \\ \quad + \boldsymbol{g_2}(\boldsymbol{x}_1, \boldsymbol{x}_2, \varepsilon^2\,\boldsymbol{y}_1, \varepsilon\boldsymbol{y}_2) + \tilde{\mathbf{K}}_w\boldsymbol{y}_1] - \mathbf{J}^{-1}\boldsymbol{u}\end{array}\right\} \tag{19}$$

Let $z_1 = \boldsymbol{y}_1 - \bar{\boldsymbol{\xi}}_q; z_2 = \boldsymbol{y}_2; z_3 = \boldsymbol{y}_1 - \bar{\boldsymbol{\xi}}_\delta; z_4 = \boldsymbol{y}_4$ be the states in the fast time-scale ($t_f = \frac{t}{\varepsilon}$) after boundary layer correction

(3). Then, substituting these in (19) gives the fast subsystem:

$$\left.\begin{array}{l}\dfrac{dz_1}{dt_f} = z_2 \\[2mm] \dfrac{dz_2}{dt_f} = -\mathbf{H_{21}}(\boldsymbol{x}_1, \varepsilon^2(\boldsymbol{z}_1 + \bar{\boldsymbol{y}}_1))[\boldsymbol{f_1}(\boldsymbol{x}_1, \boldsymbol{x}_2) \\ \quad + \boldsymbol{g_1}(\boldsymbol{x}_1, \boldsymbol{x}_2, \varepsilon^2(\boldsymbol{z}_1 + \bar{\boldsymbol{y}}_1), \varepsilon\boldsymbol{z}_2) - \tilde{\mathbf{K}}_s(\boldsymbol{z}_3 + \bar{\boldsymbol{y}}_3)] \\ \quad - \mathbf{H_{22}}(\boldsymbol{x}_1, \varepsilon^2(\boldsymbol{z}_1 + \bar{\boldsymbol{y}}_1))[\boldsymbol{f_2}(\boldsymbol{x}_1, \boldsymbol{x}_2) \\ \quad + \boldsymbol{g_2}(\boldsymbol{x}_1, \boldsymbol{x}_2, \varepsilon^2(\boldsymbol{z}_1 + \bar{\boldsymbol{y}}_1), \varepsilon\boldsymbol{z}_2) + \tilde{\mathbf{K}}_w(\boldsymbol{z}_1 + \bar{\boldsymbol{y}}_1)] \\[2mm] \dfrac{dz_3}{dt_f} = z_4 \\[2mm] \dfrac{dz_4}{dt_f} = -\{\mathbf{H_{11}}(\boldsymbol{x}_1, \varepsilon^2(\boldsymbol{z}_1 + \bar{\boldsymbol{y}}_1)) + \mathbf{J}^{-1}\}[-\tilde{\mathbf{K}}_s\boldsymbol{y}_3 \\ \quad + \boldsymbol{f_1}(\boldsymbol{x}_1, \boldsymbol{x}_2) + \boldsymbol{g_1}(\boldsymbol{x}_1, \boldsymbol{x}_2, \varepsilon^2(\boldsymbol{z}_1 + \bar{\boldsymbol{y}}_1), \varepsilon\boldsymbol{z}_2)] \\ \quad - \mathbf{H_{12}}(\boldsymbol{x}_1, \varepsilon^2(\boldsymbol{z}_1 + \bar{\boldsymbol{y}}_1))[\boldsymbol{f_2}(\boldsymbol{x}_1, \boldsymbol{x}_2) \\ \quad + \boldsymbol{g_2}(\boldsymbol{x}_1, \boldsymbol{x}_2, \varepsilon^2(\boldsymbol{z}_1 + \bar{\boldsymbol{y}}_1), \varepsilon\boldsymbol{z}_2) + \tilde{\mathbf{K}}_w(\boldsymbol{z}_1 + \bar{\boldsymbol{y}}_1)] \\ \quad - \mathbf{J}^{-1}\boldsymbol{u}\end{array}\right\} \tag{20}$$

However, at the boundary layer, $\frac{dx_1}{dt_f} = \frac{dx_2}{dt_f} = \boldsymbol{g_1}(\boldsymbol{x}_1, \boldsymbol{x}_2, \mathbf{0}, \mathbf{0}) = \boldsymbol{g_2}(\boldsymbol{x}_1, \boldsymbol{x}_2, \mathbf{0}, \mathbf{0}) = 0$, and (20) reduces to:

$$\left.\begin{array}{l}\dfrac{dz_1}{dt_f} = z_2 \\[2mm] \dfrac{dz_2}{dt_f} = -\mathbf{H_{21}}(\bar{\boldsymbol{x}}_1, \mathbf{0})\boldsymbol{f_1}(\bar{\boldsymbol{x}}_1, \bar{\boldsymbol{x}}_2) - \mathbf{H_{22}}(\bar{\boldsymbol{x}}_1, \mathbf{0})\boldsymbol{f_2}(\bar{\boldsymbol{x}}_1, \bar{\boldsymbol{x}}_2) \\ \quad - \mathbf{H_{22}}(\bar{\boldsymbol{x}}_1, \mathbf{0})\tilde{\mathbf{K}}_w\boldsymbol{z}_1 + \mathbf{H_{21}}(\bar{\boldsymbol{x}}_1, \mathbf{0})\tilde{\mathbf{K}}_s\boldsymbol{z}_3 \\ \quad - \mathbf{H_{22}}(\bar{\boldsymbol{x}}_1, \mathbf{0})\tilde{\mathbf{K}}_w\bar{\boldsymbol{y}}_1 + \mathbf{H_{21}}(\bar{\boldsymbol{x}}_1, \mathbf{0})\tilde{\mathbf{K}}_s\bar{\boldsymbol{y}}_3 \\[2mm] \dfrac{dz_3}{dt_f} = z_4 \\[2mm] \dfrac{dz_4}{dt_f} = \mathbf{H_{11}}(\bar{\boldsymbol{x}}_1, \mathbf{0})\boldsymbol{f_1}(\bar{\boldsymbol{x}}_1, \bar{\boldsymbol{x}}_2) + \mathbf{H_{12}}(\bar{\boldsymbol{x}}_1, \mathbf{0})\boldsymbol{f_2}(\bar{\boldsymbol{x}}_1, \bar{\boldsymbol{x}}_2) \\ \quad + \mathbf{H_{12}}(\bar{\boldsymbol{x}}_1, \mathbf{0})\tilde{\mathbf{K}}_w\boldsymbol{z}_1 - \{\mathbf{H_{11}}(\bar{\boldsymbol{x}}_1, \mathbf{0}) + \mathbf{J}^{-1}\}\tilde{\mathbf{K}}_s\boldsymbol{z}_3 \\ \quad - \mathbf{J}^{-1}\boldsymbol{u}\end{array}\right\} \tag{21}$$

Substituting $\boldsymbol{\xi}_q = \boldsymbol{y}_1$ and $\boldsymbol{\xi}_\delta = \boldsymbol{y}_3$ in (13–14):

$$\bar{\boldsymbol{y}}_1 = \tilde{\mathbf{K}}_w^{-1}\mathbf{H_{22}^{-1}}(\bar{\theta}, \mathbf{0})[-\mathbf{H_{21}}(\bar{\theta}, \mathbf{0})\boldsymbol{f_1}(\bar{\theta}, \dot{\bar{\theta}})$$
$$- \mathbf{H_{22}}(\bar{\theta}, \mathbf{0})\boldsymbol{f_2}(\bar{\theta}, \dot{\bar{\theta}}) + \mathbf{H_{21}}(\bar{\theta}, \mathbf{0})\tilde{\mathbf{K}}_s\bar{\boldsymbol{y}}_3] \tag{22}$$
$$\bar{\boldsymbol{y}}_3 = \tilde{\mathbf{K}}_s^{-1}\{\mathbf{H_{11}}(\bar{\theta}, \mathbf{0}) - \mathbf{H_{12}}(\bar{\theta}, \mathbf{0})\mathbf{H_{22}^{-1}}(\bar{\theta}, \mathbf{0})\mathbf{H_{21}}(\bar{\theta}, \mathbf{0}) + \mathbf{J}^{-1}\}^{-1}$$
$$\times \left[(\mathbf{H_{11}}(\bar{\theta}, \mathbf{0}) - \mathbf{H_{12}}(\bar{\theta}, \mathbf{0})\mathbf{H_{22}^{-1}}(\bar{\theta}, \mathbf{0})\mathbf{H_{21}}(\bar{\theta}, \mathbf{0}))\boldsymbol{f_1}(\bar{\theta}, \dot{\bar{\theta}})\right.$$
$$+ \mathbf{J}^{-1}\bar{\boldsymbol{u}}\bigg] \tag{23}$$

Using $\bar{\boldsymbol{y}}_1$ and $\bar{\boldsymbol{y}}_3$ from (22, 23) in (21):

$$\left.\begin{array}{l}\dfrac{dz_1}{dt_f} = z_2 \\[2mm] \dfrac{dz_2}{dt_f} = -\mathbf{H_{22}}(\bar{\boldsymbol{x}}_1, \mathbf{0})\tilde{\mathbf{K}}_w\boldsymbol{z}_1 + \mathbf{H_{21}}(\bar{\boldsymbol{x}}_1, \mathbf{0})\tilde{\mathbf{K}}_s\boldsymbol{z}_3 \\[2mm] \dfrac{dz_3}{dt_f} = z_4 \\[2mm] \dfrac{dz_4}{dt_f} = \mathbf{H_{12}}(\bar{\boldsymbol{x}}_1, \mathbf{0})\tilde{\mathbf{K}}_w\boldsymbol{z}_1 - \{\mathbf{H_{11}}(\bar{\boldsymbol{x}}_1, \mathbf{0}) + \mathbf{J}^{-1}\}\tilde{\mathbf{K}}_s\boldsymbol{z}_3 \\ \quad + \mathbf{J}^{-1}(\boldsymbol{u} - \bar{\boldsymbol{u}})\end{array}\right\} \tag{24}$$
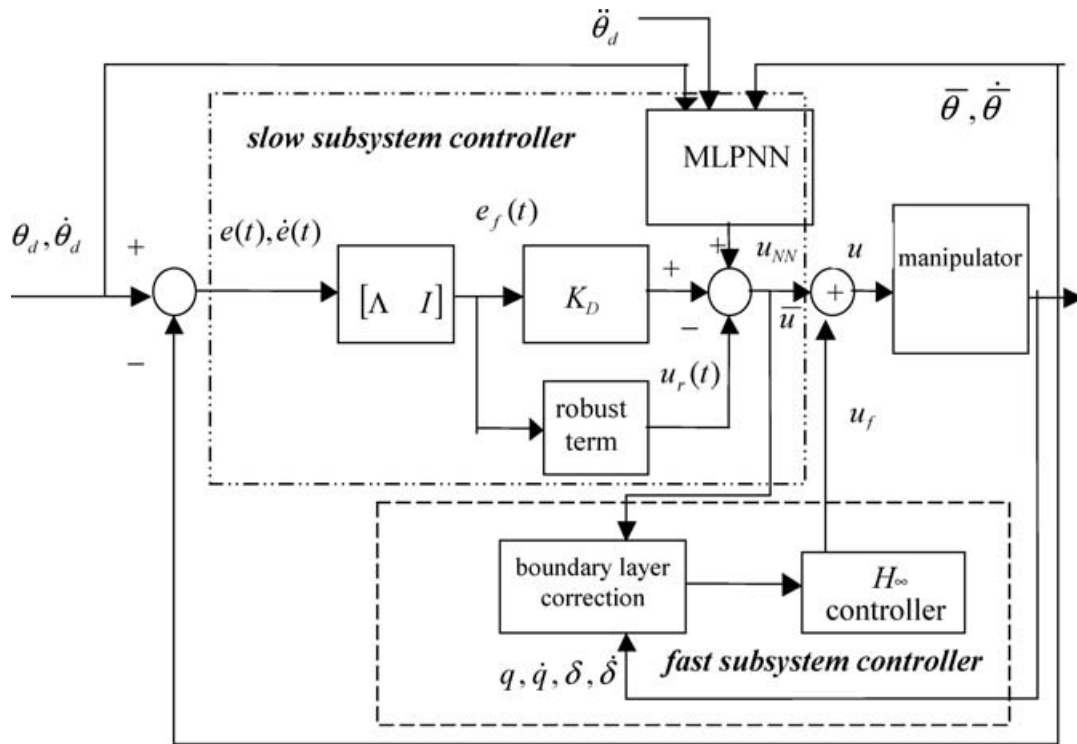
Fig. 2. Structure of the neuro-H_∞ controller.

Therefore, from (24), the fast subsystem is:

$$\dot{x}_f = \mathbf{A_f} x_f + \mathbf{B_f} u_f \qquad (25)$$

where

$$\mathbf{A_f} = \begin{bmatrix} \mathbf{0} & \mathbf{0} & \mathbf{I} \\ -\mathbf{H}_{22}\tilde{\mathbf{K}}_{\mathbf{w}} & \mathbf{H}_{21}\tilde{\mathbf{K}}_{\mathbf{s}} & \mathbf{0} \\ \mathbf{H}_{12}\tilde{\mathbf{K}}_{\mathbf{w}} & (\mathbf{H}_{11}+\mathbf{J}^{-1})\tilde{\mathbf{K}}_{\mathbf{s}} & \mathbf{0} \end{bmatrix}, \quad \mathbf{B_f} = \begin{bmatrix} \mathbf{0} \\ \mathbf{J}^{-1} \end{bmatrix};$$

$$x_f = \begin{bmatrix} z_1^T & z^T & z_2^T & z_4^T \end{bmatrix}^T, \quad u_f = u - \bar{u}$$

and $\mathbf{0}$ and $\mathbf{I}$ are zero and identity matrices.

III. SPT-BASED COMPOSITE CONTROLLER USING NEURAL NETWORK AND H∝ TECHNIQUES

In the case of a manipulator with many flexible links and joints, the dynamic equations involve a set of highly non-linear and coupled partial differential equations, thus posing a difficult control problem compared to a simple single flexible arm. A neural network based controller is likely to perform better than an inverse dynamics scheme in controlling the slow dynamics since it does not require exact knowledge of either the system dynamics or the inverse dynamic model evaluation. Furthermore, it guarantees boundedness in the tracking errors and control signals.

With regard to the fast subsystem, the H_∞ control strategy has previously been applied successfully to flexible manipulators assuming linear dynamics.[5] More recent work[6] utilised the robust features of H_∞ optimal control to stabilize

the fast subsystem in the presence of model uncertainty due to unmodelled high frequency modes, but because the standard H_∞ optimal control problem is solved for two Riccati equations i.e. one for the controller and the other for the observer, the order of the controller increases. This increases the computation time of the control task. Consequently, a state feedback H_∞ controller for the fast subsystem is proposed in this work where only one Riccati equation has to be solved, which is a special case of the standard H_∞ problem with static gains.

The structure of the new singular perturbation based, neuro-H_∞ controller (SNHC) proposed is given in Fig. 2. This is a composite controller with separate schemes for the slow and fast subsystems.

III.1. NN controller for slow subsystem
The slow dynamics (16) can be re-written after pre-multiplying both sides by $(\mathbf{M}_{11} + \mathbf{J})$ to give

$$(\mathbf{M}_{11} + \mathbf{J})\ddot{\bar{\theta}} = -f_1(\bar{\theta}, \dot{\bar{\theta}}) + \bar{u} \qquad (26)$$

Incorporating a disturbance term P_d to account for the unmodelled dynamics due to the neglected high frequency modes and higher manifold terms, the slow subsystem can be rewritten as

$$\mathbf{M_s}\ddot{\bar{\theta}} + \mathbf{C_s}(\bar{\theta}, \dot{\bar{\theta}})\dot{\bar{\theta}} + P_d = \bar{u} \qquad (27)$$

where $\mathbf{M_s} = \mathbf{M}_{11}(\theta, \mathbf{0}) + \mathbf{J}$ and $\mathbf{C_s}(\bar{\theta}, \dot{\bar{\theta}})\dot{\bar{\theta}} = f_1(\bar{\theta}, \dot{\bar{\theta}})$. Let $\theta_d(t) \in \Re^n$ be a desired trajectory, which is assumed to be at least twice differentiable. Now, consider a trajectory tracking

error defined as

$$e(t) = \boldsymbol{\theta}_d(t) - \bar{\boldsymbol{\theta}}(t) \tag{28}$$

Then, the filtered tracking error can be written as

$$\boldsymbol{e}_f(t) = \dot{\boldsymbol{e}}(t) + \boldsymbol{\Lambda} \boldsymbol{e}(t) \tag{29}$$

where $\boldsymbol{\Lambda}$ is a symmetric positive definite constant matrix. Using the filtered error from (29), the slow dynamics given in (27) can be rewritten as

$$\mathbf{M_s} \dot{\boldsymbol{e}}_f = -\mathbf{C_s} \boldsymbol{e}_f - \bar{\boldsymbol{u}} + \boldsymbol{f}(\boldsymbol{x}) + \boldsymbol{P}_d \tag{30}$$

where $\boldsymbol{f}(\boldsymbol{x})$ is the non-linear function (dynamics of the slow subsystem) given by

$$\boldsymbol{f}(\boldsymbol{x}) = \mathbf{M_s}(\ddot{\boldsymbol{\theta}}_d + \boldsymbol{\Lambda}\dot{\boldsymbol{e}}) + \mathbf{C_s}(\dot{\boldsymbol{\theta}}_d + \boldsymbol{\Lambda} e) + \boldsymbol{P}_d \tag{31}$$

with $x = [\boldsymbol{e}^T \ \dot{\boldsymbol{e}} \ \boldsymbol{\theta}_d^T \ \dot{\boldsymbol{\theta}}_d^T \ \ddot{\boldsymbol{\theta}}_d^T]^T$.
The unknown function $\boldsymbol{f}(\boldsymbol{x})$ can be approximated by applying a three-layer NN such that:[7]

$$\boldsymbol{f}(\boldsymbol{x}) = \mathbf{W^T} \boldsymbol{a}(\mathbf{V^T} \boldsymbol{x}) + \Xi \tag{32}$$

where $\boldsymbol{a}(\boldsymbol{x})$ is a sigmoidal activation function, $\mathbf{W}$ and $\mathbf{V}$ are respectively the ideal connection weights for the *input layer to hidden layer* and *hidden layer to output layer* and Ξ is the function approximation error.

The NN estimate of $\boldsymbol{f}(x)$ is:

$$\hat{\boldsymbol{f}}(\boldsymbol{x}) = \hat{\mathbf{W}}^\mathbf{T} \boldsymbol{a}(\hat{\mathbf{V}}^\mathbf{T} \boldsymbol{x}) \tag{33}$$

where $\hat{\mathbf{V}}$ and $\hat{\mathbf{W}}$ are the actual NN weights.

Now, define a control input vector for the slow dynamics based on the function approximation as:

$$\bar{\boldsymbol{u}}(t) = \hat{\boldsymbol{f}}(\boldsymbol{x}) + \mathbf{K_D} \boldsymbol{e}_f - \boldsymbol{u}_r(t) \tag{34}$$

where $\mathbf{K_D}$ is a positive gain matrix and $\boldsymbol{u}_r(t)$ provides robustness in the face of higher-order terms in the Taylor series. Substituting for $\hat{\boldsymbol{f}}$ from (33) in (34) gives

$$\bar{\boldsymbol{u}} = \hat{\mathbf{W}}^\mathbf{T} \boldsymbol{a}(\hat{\mathbf{V}}^\mathbf{T} \boldsymbol{x}) + \mathbf{K_D} \boldsymbol{e}_f - \boldsymbol{u}_r(t) \tag{35}$$

Substituting (35) in (30), the inner slow control system becomes

$$\mathbf{M_s} \dot{\boldsymbol{e}}_f(t) = -(\mathbf{K_D} + \mathbf{C_s}) \boldsymbol{e}_f(t) + \mathbf{W^T} \boldsymbol{a}(\hat{\mathbf{V}} \boldsymbol{x})$$
$$- \hat{\mathbf{W}}^T \boldsymbol{a}(\hat{\mathbf{V}} \boldsymbol{x}) + \Xi + \boldsymbol{P}_d + \boldsymbol{u}_r(t) \tag{36}$$

Some further manipulation yields:

$$\mathbf{M_s} \dot{\boldsymbol{e}}_f(t) = -(\mathbf{K_D} + \mathbf{C_s}) \boldsymbol{e}_f(t) + \tilde{\mathbf{W}}^\mathbf{T} \hat{\boldsymbol{a}} + \hat{\mathbf{W}}^\mathbf{T} \tilde{\boldsymbol{a}}$$
$$+ \tilde{\mathbf{W}}^\mathbf{T} \tilde{\boldsymbol{a}} + \boldsymbol{w}(t) + \boldsymbol{u}_r(t) \tag{37}$$

where:

$\tilde{\mathbf{W}} = \mathbf{W} - \hat{\mathbf{W}}$, $\hat{\boldsymbol{a}}$ is the hidden layer output error given by:[7]

$$\tilde{\boldsymbol{a}} = \boldsymbol{a} - \hat{\boldsymbol{a}} = \boldsymbol{a}(\mathbf{V^T} \boldsymbol{x}) - \boldsymbol{a}(\hat{\mathbf{V}}^\mathbf{T} \boldsymbol{x})$$

and $\boldsymbol{w}(t) = \tilde{\mathbf{W}}^\mathbf{T} \hat{\boldsymbol{a}}' \mathbf{V^T} \boldsymbol{x} + \mathbf{W^T} O(\tilde{\mathbf{V}}^\mathbf{T} \boldsymbol{x})^2 + (\Xi + \boldsymbol{P}_d)$ which is bounded by

$$\boldsymbol{w}(t) \le c_0 + c_1 \|\tilde{\mathbf{Z}}\| + c_2 \|x\| \|\mathbf{Z}\| \tag{38}$$

c_0, c_1 and c_2 denote positive constants.

The tuning algorithm for the weights of the NN used to give slow control action is an unsupervised back propagation through time scheme with zero initial weights and no off-line learning phase. Control action is performed by the PD loop to keep the system stable until the NN begins to learn. The weights are tuned on-line in real-time as the system tracks the desired trajectory. The tracking performance improves as the NN learns $\boldsymbol{f}(x) \cdot \boldsymbol{u}_r$ is chosen as

$$\boldsymbol{u}_r = -\mathbf{K_z}(\|\hat{\mathbf{Z}}\|_F + \mathbf{Z}_M) \boldsymbol{e}_f(t) \tag{39}$$

where $\mathbf{K_z} > c_2$. Consider the weights for the NN to be tuned on-line using the following adaptation algorithm as

$$\left.\begin{array}{l} \dot{\hat{\mathbf{W}}}^\mathbf{T} = \mathbf{G_1} \hat{\boldsymbol{a}} \, \boldsymbol{e}_f^T(t) - \mathbf{G_1} \hat{\boldsymbol{a}}' \mathbf{V^T} \boldsymbol{x} \, \boldsymbol{e}_f^T(t) - k_d \, \mathbf{G_1} \|\boldsymbol{e}_f(t)\| \, \hat{\mathbf{W}} \\[2mm] \dot{\hat{\mathbf{V}}}^\mathbf{T} = \mathbf{G_2} \boldsymbol{x}(\hat{\boldsymbol{a}}' \hat{\mathbf{W}} \, \boldsymbol{e}_f(t))^T - k_d \mathbf{G_2} \|\boldsymbol{e}_f(t)\| \, \hat{\mathbf{V}} \end{array}\right\}$$
$$\tag{40}$$

where $\mathbf{G_1}$ and $\mathbf{G_2}$ are constant positive diagonal matrices and $k_d > 0$ is a design parameter. Inputs to the NN consist of derivative position error, whereas the back-propagation law uses the error between the desired NN output and the actual NN output.

III.2. H_∞ controller for fast subsystem

Referring to equations (17, 18), the following can be defined:

$$\left.\begin{array}{l} \mathbf{A}_1(\boldsymbol{x}_1, \boldsymbol{x}_2, \varepsilon^2 \boldsymbol{y}_1, \varepsilon \, \boldsymbol{y}_2) = -\mathbf{H}_{11}(\boldsymbol{x}_1, \varepsilon^2 \boldsymbol{y}_1)[\boldsymbol{f}_1 + \boldsymbol{g}_1] \\ \qquad\qquad\qquad\qquad -\mathbf{H}_{12}(\boldsymbol{x}_1, \varepsilon^2 \boldsymbol{y}_1)[\boldsymbol{f}_2 + \boldsymbol{g}_2] \\[1mm] \mathbf{A}_2(\boldsymbol{x}_1, \boldsymbol{x}_2, \varepsilon^2 \boldsymbol{y}_1, \varepsilon \, \boldsymbol{y}_2) = -\mathbf{H}_{21}(\boldsymbol{x}_1, \varepsilon^2 \boldsymbol{y}_1)[\boldsymbol{f}_1 + \boldsymbol{g}_1] \\ \qquad\qquad\qquad\qquad -\mathbf{H}_{22}(\boldsymbol{x}_1, \varepsilon^2 \boldsymbol{y}_1)[\boldsymbol{f}_2 + \boldsymbol{g}_2] \\[1mm] \mathbf{A}_3(\boldsymbol{x}_1, \varepsilon^2 \boldsymbol{y}_1) = \mathbf{H}_{11}(\boldsymbol{x}_1, \varepsilon^2 \boldsymbol{y}_1) \tilde{\mathbf{K}}_\mathbf{s} \\[1mm] \mathbf{A}_4(\boldsymbol{x}_1, \varepsilon^2 \boldsymbol{y}_1) = \mathbf{H}_{21}(\boldsymbol{x}_1, \varepsilon^2 \boldsymbol{y}_1) \tilde{\mathbf{K}}_\mathbf{s} \\[1mm] \mathbf{A}_5(\boldsymbol{x}_1, \varepsilon^2 \boldsymbol{y}_1) = \mathbf{H}_{12}(\boldsymbol{x}_1, \varepsilon^2 \mathbf{y}_1) \tilde{\mathbf{K}}_\mathbf{w} \\[1mm] \mathbf{A}_6(\boldsymbol{x}_1, \varepsilon^2 \boldsymbol{y}_1) = \mathbf{H}_{22}(\boldsymbol{x}_1, \varepsilon^2 \mathbf{y}) \tilde{\mathbf{K}}_\mathbf{w} \\[1mm] \mathbf{A}_7(\boldsymbol{x}_1, \varepsilon^2 \boldsymbol{y}_1) = (\mathbf{H}_{11}(\mathbf{x_1}, \varepsilon^2 \mathbf{y}) + \mathbf{J}^{-1}) \tilde{\mathbf{K}}_\mathbf{w} \end{array}\right\}$$
$$\tag{41}$$

Using (41) and incorporating the disturbance effects due to neglecting the higher order manifold terms, the augmented fast subsystem can be rewritten as

$$\dot{\boldsymbol{x}}_f = \mathbf{A_f} \boldsymbol{x}_f + \mathbf{B_w} \boldsymbol{w}_f + \mathbf{B_f} \boldsymbol{u}_f \tag{42}$$

where the subsystem matrices are given by

$$\mathbf{A_f} = \begin{bmatrix} \mathbf{0} & \mathbf{0} & \mathbf{I} \\ -\mathbf{A_6} & \mathbf{A_4} & \mathbf{0} \\ \mathbf{A_5} & \mathbf{A_7} & \mathbf{0} \end{bmatrix}, \quad \mathbf{B_f} = \begin{bmatrix} \mathbf{0} \\ \mathbf{J^{-1}} \end{bmatrix}; \quad \mathbf{B_w} = \begin{bmatrix} \mathbf{0} & \mathbf{0} & \mathbf{I} \\ \Delta_1 & \Delta_2 & \mathbf{0} \\ \Delta_3 & \Delta_4 & \mathbf{0} \end{bmatrix};$$
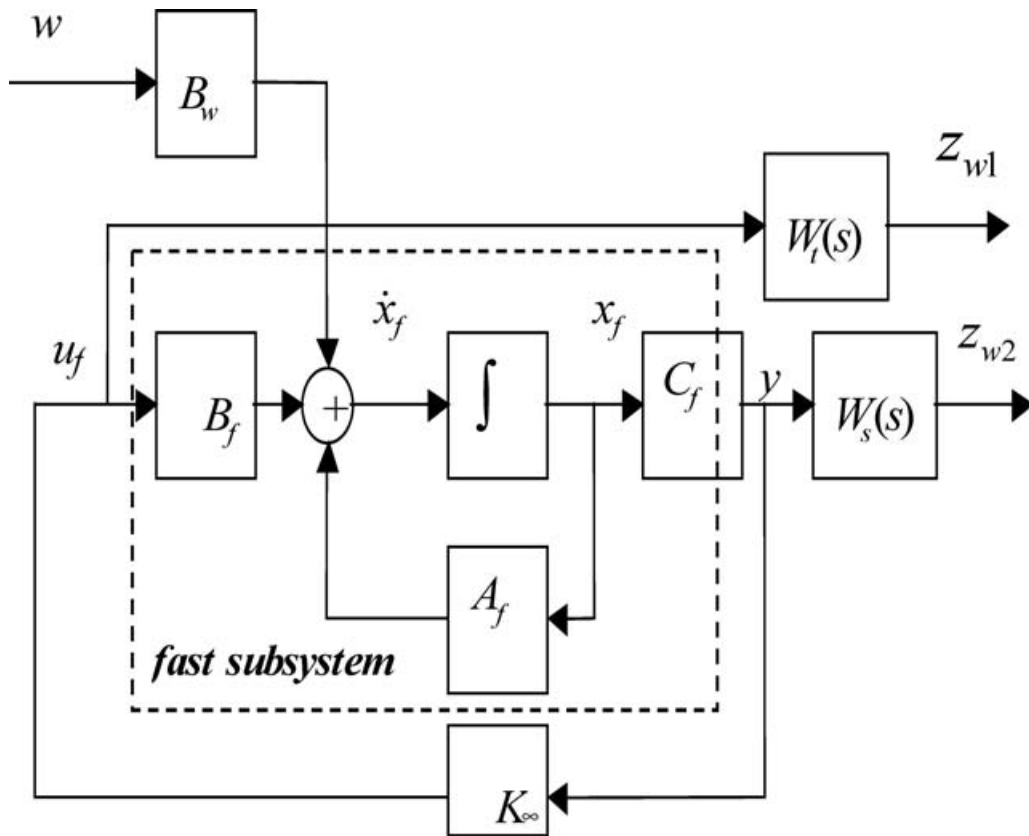
Fig. 3. Structure of the fast controller.

and the states are: $x_f = [z_1^T \; z_3^T \; z_2^T \; z_4^T]^T$, the disturbance vector is $w_f = [w_1 \; w_2 \; \cdot \; w_n]$; Δ_1, Δ_2, Δ_3 and Δ_4 denote the neglected higher manifold expansion contributions.

Fig. 3 gives the structure of the $\boldsymbol{H}_\infty -$ based fast subsystem controller, in which weighting functions $\mathbf{W_t}(s)$, $\mathbf{W_s}(s)$ are selected such that the output is immune to disturbances in the low frequency range and high frequency robustness is guaranteed. Typically, $\mathbf{W_t}(s)$ and $\mathbf{W_s}(s)$ are low and high pass filters, respectively. Representing the unmodelled dynamics due to neglecting the high frequency modes as an output multiplicative uncertainty, the perturbed system can be expressed as

$$\mathbf{G_{fl}(s)} = \mathbf{G_{fn}(s)}(\mathbf{I} + \mathbf{G_m(s)}) \tag{43}$$

where $\mathbf{G_{fl}}(s)$, $\mathbf{G_{fn}}(s)$ and $\mathbf{G_m}(s)$ are the transfer functions of the perturbed system, reduced order system and the multiplicative uncertainty respectively. Robust stability will be achieved if the following norm inequality holds

$$\|\mathbf{G_m(s)T(s)}\|_\infty < 1 \tag{44}$$

where $\mathbf{T(s)}$ is the transfer function from the disturbance w_f to the control input u_f. Due to difficulty in representing the uncertainty exactly, $\mathbf{W_t}(s)$ is selected to cover the upper bound of the uncertainty in the entire frequency range, i.e.

$$\bar{\sigma}(\mathbf{G_m}(j\omega)) \leq \mathbf{W_t}(j\omega) \quad \forall \omega \tag{45}$$

where $\bar{\sigma}(\cdot)$ is the singular value, ω is the frequency. Therefore, (44) can be rewritten as

$$\|\mathbf{W_t(s)T(s)}\|_\infty < 1 \tag{46}$$

To improve the system performance such that the effects of the disturbances on the output are reduced, the controller must satisfy the following criteria

$$\|\mathbf{W_s(s)S(s)}\|_\infty < 1 \tag{47}$$

where $\mathbf{S}(s)$ is the transfer function between w_f and y. The specifications expressed in (44) to (47) are achieved by designing a controller $\mathbf{K}_\infty(\mathbf{s})$ that satisfies the following mixed sensitivity criteria:

$$\left\| \begin{matrix} \mathbf{W_t(s)T(s)} \\ \mathbf{W_s(s)S(s)} \end{matrix} \right\|_\infty < 1 \tag{48}$$

If these weighting transfer functions are written in state space form as: $\mathbf{W_t(s)} = \mathbf{C_{wt}(sI - A_{wt})^{-1}}$ and $\mathbf{W_s(s)} = \mathbf{C_{ws}(sI - A_{ws})^{-1}}$, then, referring to Fig. 3, the augmented fast subsystem can be written as

$$\left. \begin{aligned} \dot{x}_g &= \mathbf{A_g} x_g + \mathbf{B_{g1}} w_f + \mathbf{B_{g2}} u_f \\ z &= \mathbf{C_{g1}} x_g + \mathbf{D_{g12}} u_f \\ y_g &= \mathbf{C_{g2}} x_g \end{aligned} \right\} \tag{49}$$

where the augmented state vector is: $x_g = [x_f \ x_{wt} \ x_{ws}]^T$, and the states of the augmented system are:

$$\mathbf{A_g} = \begin{bmatrix} \mathbf{A_f} & \mathbf{0} & \mathbf{0} \\ \mathbf{0} & \mathbf{A_{wt}} & \mathbf{0} \\ \mathbf{D_{ws}C_f} & \mathbf{0} & \mathbf{A_{ws}} \end{bmatrix}; \quad \mathbf{B_{g1}} = \begin{bmatrix} \mathbf{B_w} \\ \mathbf{0} \\ \mathbf{0} \end{bmatrix}; \quad \mathbf{B_{g2}} = \begin{bmatrix} \mathbf{B_f} \\ \mathbf{B_{wt}} \\ \mathbf{0} \end{bmatrix};$$

$$\mathbf{C_{g1}} = \begin{bmatrix} \mathbf{0} & \mathbf{C_{wt}} & \mathbf{0} \\ \mathbf{D_{ws}C_f} & \mathbf{0} & \mathbf{C_{ws}} \end{bmatrix}; \quad \mathbf{D_{g12}} = \begin{bmatrix} \mathbf{D_{wt}} \\ \mathbf{0} \end{bmatrix}.$$

The objective of the state feedback H_∞ controller is to find a constant gain matrix, $\mathbf{K_\infty}$ such that the state feedback control law

$$u_f = \mathbf{K_\infty} x_g \qquad (50)$$

stabilizes the augmented uncertain linear system given in (49) and satisfies $\|\mathbf{T_{zw}}\|_\infty \le 1$, where $\|\mathbf{T_{zw}(s)}\|_\infty$ is the closed loop transfer function matrix between w_f and z_w and the closed-loop fast subsystem matrix $(\mathbf{A_g} - \mathbf{B_{g2}K_\infty})$ is stable. Therefore, to find a state feedback controller such that $\|\mathbf{T_{zw}(s)}\|_\infty \le 1$, it is necessary to find a positive definite matrix $\mathbf{P_\infty}$ that satisfies

$$(\mathbf{A_g} + \mathbf{B_{g2}K_\infty})^T \mathbf{P_\infty} + \mathbf{P_\infty}(\mathbf{A_g} + \mathbf{B_{g2}K_\infty}) + (\mathbf{C_{g1}} + \mathbf{D_{g12}K_\infty})^T$$
$$\times (\mathbf{C_{g1}} + \mathbf{D_{g12}K_\infty}) + \mathbf{P_\infty}\mathbf{B_{g1}}\mathbf{B_{g1}}^T \mathbf{P_\infty} = \mathbf{0} \qquad (51)$$

Defining $\mathbf{\Pi} = \mathbf{D_{12}}^T \mathbf{D_{12}}$ and $\mathbf{\Sigma} = \mathbf{D_{g12}}^T \mathbf{C_{g1}} + \mathbf{B_{g2}}\mathbf{P_\infty}$ and substituting these in (51):

$$\mathbf{A_g}^T \mathbf{P_\infty} + \mathbf{P_\infty}\mathbf{A_g} + \mathbf{C_{g1}}^T \mathbf{C_{g1}} - \mathbf{\Sigma}^{-1}\mathbf{\Pi}\mathbf{\Sigma} + \mathbf{P_\infty}\mathbf{B_{g1}}\mathbf{B_{g1}}^T \mathbf{P_\infty}$$
$$+ (\mathbf{K_\infty} + \mathbf{\Sigma}^{-1}\mathbf{\Pi})^T \mathbf{\Pi}(\mathbf{K_\infty} + \mathbf{\Sigma}\mathbf{\Pi}) = \mathbf{0} \qquad (52)$$

Now assuming $\mathbf{K_\infty} = -\mathbf{\Pi}^{-1}\mathbf{\Sigma}$ in (52):

$$\mathbf{A_g}^T \mathbf{P_\infty} + \mathbf{P_\infty}\mathbf{A_g} + \mathbf{C_{g1}}^T \mathbf{C_{g1}} - \mathbf{\Sigma}^{-1}\mathbf{\Pi}\mathbf{\Sigma} + \mathbf{P_\infty}\mathbf{B_{g1}}\mathbf{B_{g1}}^T \mathbf{P_\infty} = \mathbf{0}$$
$$(53)$$

Then the state feedback controller is given by[8]

$$u_f = \mathbf{K_\infty} x_g \quad \text{where} \quad \mathbf{K_\infty} = -\mathbf{B_{g2}}^T \mathbf{P_\infty} \qquad (54)$$

Let x_m be the vector of available states, which can be written as a linear combination of the augmented state variables x_g as

$$x_m = \mathbf{L} x_g \qquad (55)$$

where $\mathbf{L}$ is a constant matrix. Let the control input in terms of x_m be expressed as

$$u_f = \mathbf{K_m} x_m \qquad (56)$$

Substituting x_m from (55) in (56) gives

$$u_f = \mathbf{K_m} \mathbf{L} x_g \qquad (57)$$

But the control based on the full state feedback is

$$u_f = \mathbf{K_\infty} x_g \qquad (58)$$

Therefore, using (56, 58), the gains $\mathbf{K_m}$ can be computed from the full state gain matrix by minimising the matrix norm $\|(\mathbf{K_\infty} - \mathbf{K_m}\mathbf{L})^{-1}\|_\infty$ to give a mean square solution given by[9]

$$\mathbf{K_m} = \mathbf{K_\infty} \mathbf{L}^T (\mathbf{L}\mathbf{L}^T)^{-1} \qquad (59)$$

III.3. Stability of composite controller

For the slow subsystem, it may be noted that $\{\dot{\mathbf{M}}_s - 2\mathbf{C}_s\}$ is skew-symmetric as in the case of rigid manipulators. Therefore, by using this symmetric property in $\{\dot{\mathbf{M}}_s - 2\mathbf{C}_s\}$, it can be shown[7] that the stability of the resulting slow NN controller with the tuning rules (40) is guaranteed. It has also been shown in section 3.2 that robust stability of the fast subsystem is achieved by using the proposed state-feedback H_∞ controller.[8] It can then be shown (see Appendix 1) that, if both the slow subsystem and the fast subsystem are asymptotically stable, then the overall system (full-order system) is ultimately stable.

IV. RESULTS AND DISCUSSION

Simulations were performed to compare the performance of the new SNHC algorithm with the alternative SPT-based inverse dynamics and linear quadratic regulator composite controller (SCLC) reported previously[3] when applied to a manipulator with two flexible-links and two flexible-joints, with both links and joints having the same parameters as specified in Table I. The manipulator was commanded to follow a desired trajectory given by

$$\boldsymbol{\theta}_d(t) = \boldsymbol{\theta}_0(t) + \left(6\frac{t^5}{t_d^5} - 15\frac{t^4}{t_d^4} + 10\frac{t^3}{t_d^3}\right)(\boldsymbol{\theta}_f - \boldsymbol{\theta}_0);$$

where $\boldsymbol{\theta}_d(t) = [\theta_{d1}(t) \ \theta_{d2}(t)]^T$ are the desired link trajectories, $\boldsymbol{\theta}_0 = [0 \ 0]^T$ are the initial link positions, $\boldsymbol{\theta}_f = [\frac{\pi}{2} \ \frac{\pi}{6}]^T$

Table I. Parameters of the manipulator links and joints.

Parameter	Symbol	*Value*
Mass density	ρ	0.2 kg m^{-1}
Flexural rigidity	EI	1.0 Nm^2
Length	l	0.5 m
Rotor and hub Inertia	I$_r$	0.02 kg m^2
Gear ratio	G	1
Stiffness constant	k$_s$	100 Nm/rad
Payload mass	m$_p$	0.1 kg
Payload Inertia	I$_p$	0.005 kg m^2
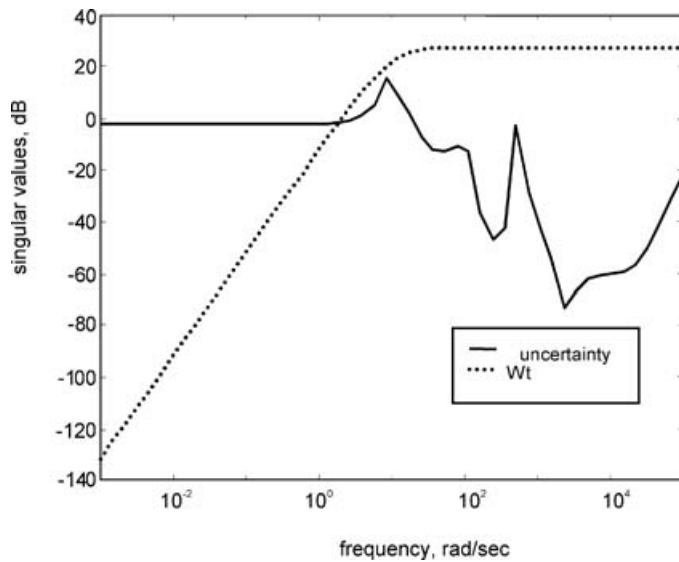
Fig. 4. Sigma plots for uncertainty and $W_t(s)$ of the fast subsystem.

Fig. 5. Comparison of tracking performances.

Fig. 6. Comparison of joint deflections.

are the final positions, t_d is the time taken along the trajectory to reach the final position which is taken as 4 seconds.

For the slow system NN controller, 10 input neurons were used corresponding to $x = [e_{2 \times 1} \; \dot{e}_{2 \times 1} \; \theta_{d2 \times 1} \; \dot{\theta}_{d2 \times 1} \; \ddot{\theta}_{d2 \times 1}]^T$. The output layer consisted of 2 nodes for the two control signals, and 10 hidden nodes were chosen. The controller parameters were set as $\mathbf{K_D} = diag(2.5, 2.5)$, $\mathbf{K_z} = diag(15.0, 15.0)$, $\mathbf{\Lambda} = diag(1.5, 1.5)$ and $\mathbf{Z_M} = 50.0$, these values having been chosen by trial and error to give small tracking errors. The weight tuning algorithm (40) was implemented by using a trapezoidal integration method with a step size of 1ms and with $\mathbf{G_1} = diag(12.0, 12.0)$, $k_d = 0.000001$ and $\mathbf{G_2} = diag(12.0, 12.0)$.

For the fast system controller, the disturbance matrix elements Δ_i, $i = 1, 2 \ldots 4$ in $\mathbf{B_w}$ (49) were set at 1% of the nominal values of the $\mathbf{A_f}$ matrix elements. (N.B. the $\mathbf{A_f}$ matrix contains the nominal values corresponding to $\varepsilon = 0$ only, without considering the higher order perturbation terms).[4] In designing the fast controller, the reduced order model used comprised of one flexible link mode and one flexible joint mode for each link. Its singular value plot is shown in Fig. 4. The neglected higher modes were considered to be an output multiplicative uncertainty whose transfer function was found using (43). The weighting matrix $\mathbf{W_t}(s)$ corresponding to two control inputs, referring to Fig. 4, was chosen as $\mathbf{W_t}(s) = diag(w_t(s), w_t(s))$, where $w_t(s) = \frac{25s^2}{(s+10)^2}$. Similarly, $\mathbf{W_s}(s)$ was selected as $\mathbf{W_s}(s) = diag(w_s(s), w_s(s), w_s(s), w_s(s))$, with $w_s(s) = \frac{5}{(s+0.01)}$. The full state feedback gains were found as $\mathbf{K}_\infty = \{2.2830, 0.9388, -0.6186, 0.7041, 12.1779, 8.4038, 7.1432, -5.4418, -22.8176, -10.3386, -0.2263, 0.0684, 44.1211, 19.8186, 19.8658, 9.1293, 30.6856, -0.0023, 0.0013, -0.0008, -0.0031, 30.6865, -0.0012, -0.0011, -27.7447, -12.7041, -0.3586, 0.4743, 1.0977, 0.4402, 0.4027, 0.0245, -2.8026, -1.2833, -0.0358, 0.0481, 0.1109, 0.0445, 0.0025\}$. The observer-based controller
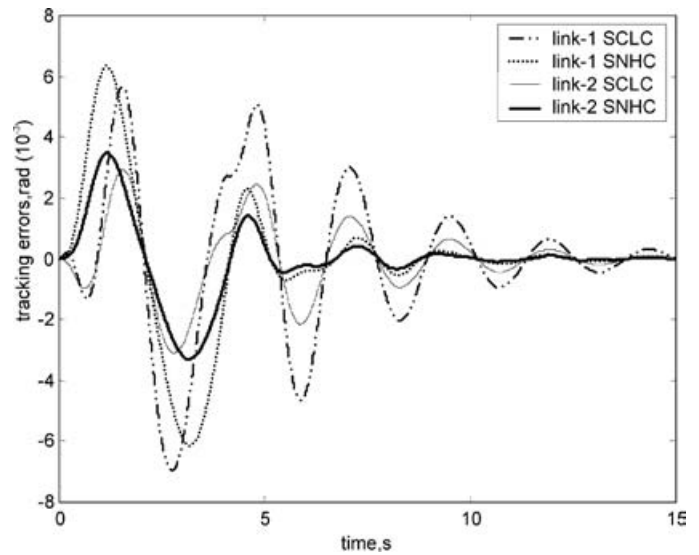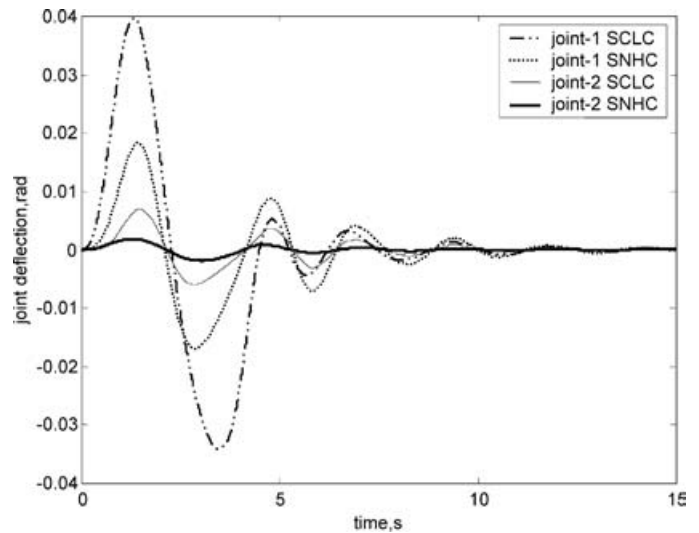
gains were determined as: $\mathbf{K}_m = \{2.2830, 0.9388, -0.6186, 0.7041, 12.1779, 8.4038, 7.1432, -5.4418, 0.1109, 0.0445, 0.0408, \text{ and } 0.0025\}$.

The performances of the SNHC and SCLC are compared in figures 5 to 10. Fig. 5 shows that, although the initial tracking errors are bigger in the case of SNHC, these become more damped and decay faster after a small time, whereas significant errors persist in the case of SCLC. It is clear from the joint deflection trajectories shown in Fig. 6 that SNHC yields smaller joint deflections and supresses them more quickly. The damping characteristics in Figs.7 and 8 show that the first and second flexible modes for both links are less excited with SNHC, leading to smaller tip deflections (Fig. 9). Figure 10 shows the control torque profiles generated by the two control schemes and it can be seen that, for both joints, the control torque magnitudes required are less for SNHC compared to SCLC.
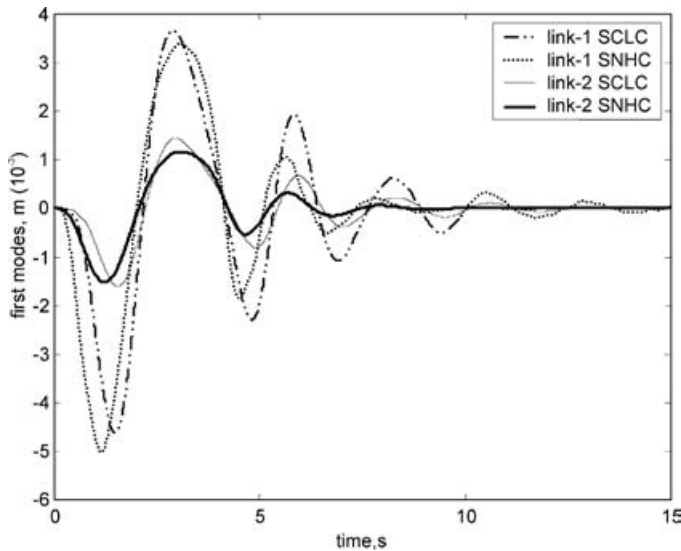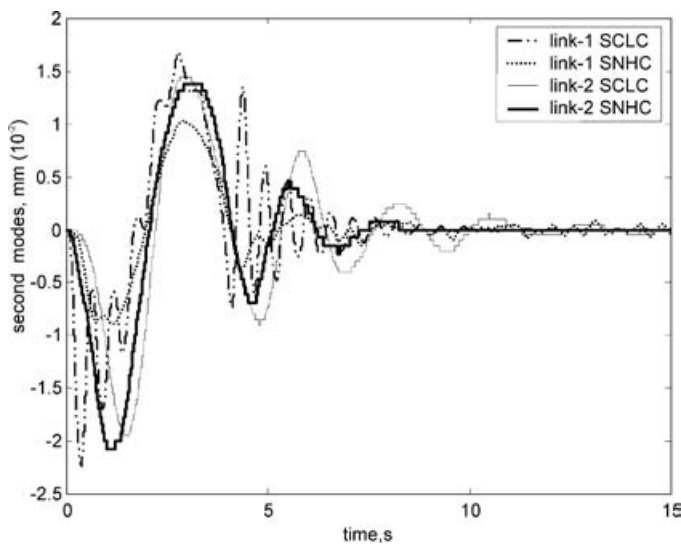
Fig. 7. Comparison of first modal vibration.

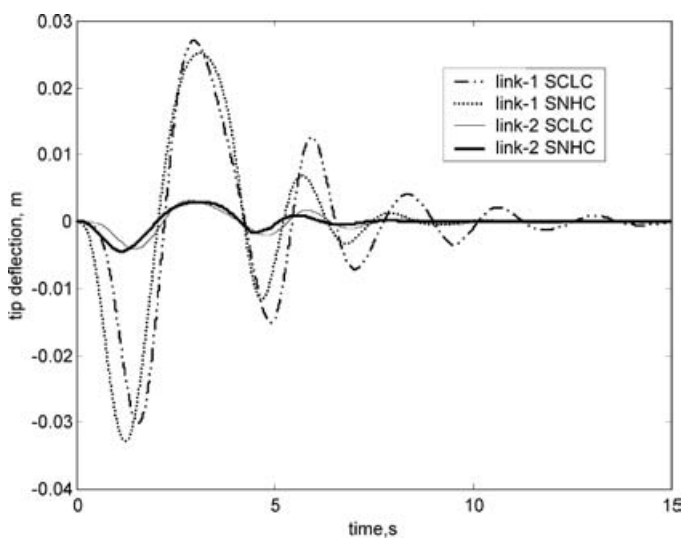Fig. 8. Comparison of second modal vibration.

Fig. 9. Comparison of tip deflection trajectories.
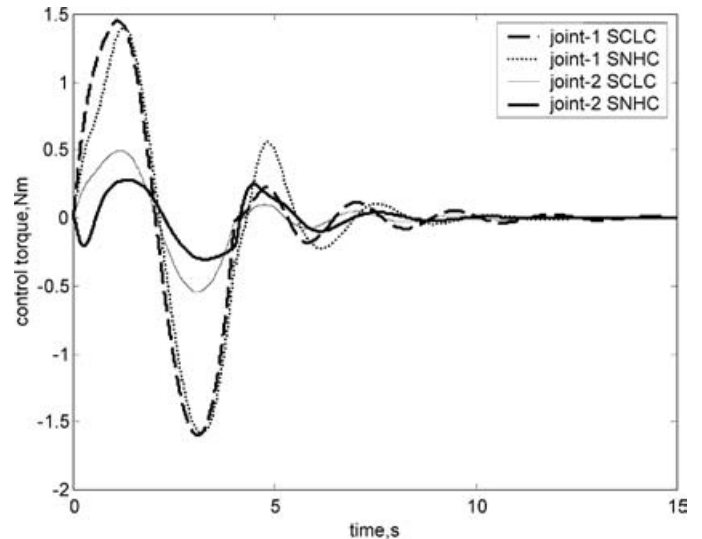

Fig. 10. Comparison of control torque profiles.

V. CONCLUSIONS

The paper has described the development of a novel neuro-$H\infty$ robust composite control scheme for a manipulator with flexible links and joints based on a two-time-scale singular perturbation model. This new neuro-H_∞ control scheme has been shown to perform better than an alternative inverse dynamics/LQR controller proposed earlier that was also based on a singular perturbation model. Improvement has been demonstrated both in trajectory tracking accuracy and also in the efficiency with which links and joint vibrations are suppressed.

The stability of the resulting two-time-scale neuro-H_∞ is ensured as both the slow and the fast subsystem controllers are stable, leading to the composite control also being stable. Also, by using a static H_∞ controller, the controller implementation is smooth and fast. Furthermore, the overall computational burden is greatly reduced by exploiting the two-time-scale separation of the complex dynamics of the flexible link and joint manipulator, as the product terms involving $(\boldsymbol{\theta}, \dot{\boldsymbol{\theta}}, \boldsymbol{q}, \dot{\boldsymbol{q}})$ do not appear in either the slow or the fast control schemes.

References
1. B. Siciliano and W. J. Book, "A singular perturbation approach to control of lightweight flexible manipulators", *Int. J. Robotics Research* **7**(4), 79–90 (1988).
2. M. W. Spong, K. Khrosani and P. V. Kokotovic, "An integral manifold approach to the feedback control of flexible joint robots", *IEEE Journal Robotics and Automation* **3**(4), 291–300 (1987).
3. B. Subudhi and A. S. Morris, "On the singular perturbation approach to control of a multi-link manipulator with flexible links and joints", *Proc. IMechE, Journal of Systems and Control Engineering* **215**(16), 587–598 (2001).
4. M. Moallem, K. Khorasani and R. Patel, "An integral manifold approach for tip-position tracking of flexible multi-link manipulators", *IEEE Trans. Robotics and Automation* **13**(6), 823–865 (1997).
5. R. N. Banavar and P. Dominic, "An LQG/H_∞ controller for a flexible manipulator", *IEEE Trans. Control System Technology* **3**(4), 409–416 (1995).

6. Y. B. Li, Z. S. Tang and L. Youfang, "Experimental study for trajectory tracking of a two-link flexible manipulator", *Int. J. Systems Science* **31**(1), 3–9 (2000).
7. F. L. Lewis, K. Liu and A. Yesildirek, "Neural net robot controller with guaranteed tracking performance", *IEEE Trans. Neural Networks* **6**(3), 703–715 (1995).
8. P. Dorato, L. Fotuna and G. Muscato, *Robust Control for Unstructured Perturbations-an Introduction* (Springer-Verlag, USA, 1992).
9. R. L. Kosut, "Suboptimal control of linear time-invariant systems subject to control structure constraints", *IEEE Trans. Automatic Control* **AC-15** (5), 557–563 (1970).

APPENDIX 1: PROOF OF STABILITY OF COMPOSITE CONTROLLER FOR TWO-TIME-SCALE SINGULARLY PERTURBED SYSTEM

Consider a two-time-scale singularly perturbed system:

$$\dot{x} = \psi(x, y, \varepsilon) \qquad (A\,1)$$

$$\varepsilon\,\dot{y} = \Phi(x, y, \varepsilon) \qquad (A\,2)$$

and assume that the origin, $x = 0$ and $y = 0$, is an isolated equilibrium point for it. Let $\Theta(x)$ be the y variable on the reduced manifold and $z = y - \Theta$ be the off-manifold co-ordinates. In the new co-ordinates, the singularly perturbed system can be written as:

$$\dot{x} = \Psi(x, z + \Theta(x)) \qquad (A\,3)$$

$$\varepsilon\,\dot{y} = \Phi(x, z + \Theta(x)) - \varepsilon\frac{\partial\Theta}{\partial x}\Psi(x, z + \Theta(x)) \quad (A\,4)$$

A two-time-scale separation of the original system (A1 and A2) yields a reduced subsystem written as:

$$\dot{x} = \Psi(x, \Theta(x)) \qquad (A\,5)$$

and a boundary layer subsystem given as:

$$\frac{dz}{dt_{fast}} = \Phi(x, z + \Theta(x)) \qquad (A\,6)$$

If these two subsystems are individually asymptotically stable, then the full-order system is stable in the sense that $|x| \to O(\varepsilon)$ and $|z| \to \Theta(\varepsilon) + O(\varepsilon)$, and there exists an upper bound for the singular perturbation parameter.

Proof:
As the slow and fast subsystems given in equations (A5 and A6) are asymptotically stable, there exists a Lyapunov function for each one. Let $L_{v1}(\bar{x})$ be a Lyapunov function for the slow subsystem (A5) such that:

$$\frac{\partial L_{v1}(x)}{\partial x}\Psi(x, \Theta(x)) \leq -\sigma_1\,\varpi_1^2(x) \qquad (A\,7)$$

where $\varpi_1^2 : \Re^m \to \Re$, is a positive definite function, i.e. $\varpi_1(0) = 0$ and $\varpi_1(x) > 0$ for all $x \in \Re^m$. Let $L_{v2}(x, z)$ be

a Lyapunov function for the fast subsystem (A6) such that:

$$\frac{\partial L_{v2}(x, z)}{\partial z}\Phi(x, z + \Theta(x)) \leq -\sigma_2\,\varpi_2^2(z) \qquad (A\,8)$$

for all $(x, z) \in \Re^m \times \Re^n$ and $\varpi_2 : \Re^n \to \Re$ is a positive definite function i.e. $\varpi_2(0) = 0$ $\varpi_2(z) > 0$ for all $z \in \Re^n$. Then consider a composite Lyapunov function as:

$$L_v(x, z) = (1 - p)L_{v1}(x) + pL_{v2}(x, z), \quad 0 < p < 1 \qquad (A\,9)$$

where p is a constant to be chosen. Taking the first time derivative of the composite Lyapunov function (A9) gives:

$$\dot{L}_v(x, z)$$

$$= (1 - p)\frac{\partial L_{v1}}{\partial x}\Psi(x, z + \Theta(x)) + \frac{p}{\varepsilon}\frac{\partial L_{v2}(x, z)}{\partial z}$$

$$\times \Phi(x, z + \Theta(x)) - p\frac{\partial L_{v2}(x, z)}{\partial z}\frac{\partial\Theta(x)}{\partial x}$$

$$+ p\frac{\partial L_{v2}}{\partial x}\Psi(x, z + \Theta(x))$$

$$= (1 - p)\frac{\partial L_{v1}}{\partial x}\Psi(x, z + \Theta(x)) + \frac{p}{\varepsilon}\frac{\partial L_{v2}(x, z)}{\partial z}$$

$$\times \Phi(x, z + \Theta(x)) + (1 - p)\frac{\partial L_{v1}(x, z)}{\partial y}$$

$$\times [\Psi(x, z + \Theta(x)) - \Psi(x, \Theta(x))]$$

$$+ p\left[\frac{\partial L_{v2}}{\partial x} - \frac{\partial L_{v2}}{\partial z}\frac{\partial\Theta(x)}{\partial x}\right]\Psi(x, z + \Theta(x)) \quad (A\,10)$$

In equation (A10), the first two terms denote the derivatives of $L_{v1}(x)$ and $L_{v2}(x)$ along the trajectories of the reduced and the fast subsystems. These are negative definite in x and z, respectively, as defined in equations (A8 and A9). The third and fourth terms represent the effect of interconnection between the slow and the fast dynamics that has been neglected at $\varepsilon = 0$. These two terms are in general, indefinite. The third term $\frac{\partial L_{v2}(x, z)}{\partial z}[\Psi(x, z + \Theta(x)) - \Psi(x, \Theta(x))]$ shows the effect of the deviation of (A3) from the reduced system (A5) whilst the fourth one i.e. $[\frac{\partial L_{v2}}{\partial x} - \frac{\partial L_{v2}}{\partial y}\frac{\partial\Theta(x)}{\partial x}]\Psi(x, z + \Theta(x))$ represents the effect of the deviation of (A3) from the boundary layer system (A5) as well as the effect of freezing x during the boundary-layer analysis. Let these perturbation terms satisfy:

$$\frac{\partial L_v(x, z)}{\partial z}[\Psi(x, z+\Theta(x)) - \Psi(x, \Theta(x))] \leq \sigma_1\kappa_1\varpi_1(x)\varpi_2(z) \qquad (A\,11)$$

and

$$\left[\frac{\partial L_{v2}}{\partial x} - \frac{\partial L_{v2}}{\partial z}\frac{\partial\Theta(x)}{\partial x}\right]\Psi(x, z + \Theta(x))$$

$$\leq \kappa_2\varpi_1(x)\varpi_2(z) + \vartheta\varpi_2^2(z) \qquad (A\,12)$$

for some nonnegative constants κ_1, κ_2 and ϑ. Now using inequalities (A7, A8, A11 and A12):

$$
\dot{L}_v(x, z) \leq -(1-p)\sigma_1 \varpi_1^2(x) - \frac{p}{\varepsilon}\sigma_2 \varpi_2^2(z) + (1-p)
$$

$$
\times \kappa_1 \varpi_1(x)\varpi_1(x) + p\vartheta \varpi_2^2(z) = -\varpi^T(x, z)\nu\varpi(x, z)
$$

$$
\text{(A 13)}
$$

where

$$
\varpi(x, z) = \begin{bmatrix} \varpi_1(x) \\ \varpi_2(z) \end{bmatrix}
$$

and

$$
\nu = \begin{bmatrix} (1-p)\sigma_1 & -\frac{1}{2}(1-p)\kappa_1 - \frac{1}{2}p\kappa_2 \\[2ex] -\frac{1}{2}(1-p)\kappa_1 - \frac{1}{2}p\kappa_2 & p\left(\frac{\sigma}{\varepsilon} - \vartheta\right) \end{bmatrix}
$$

It may be noted that the right hand side of the inequality in equation (A13) is a quadratic form in ϖ which is negative definite when:

$$
p(1-p)\sigma_1 \left(\frac{\sigma_2}{\varepsilon} - \nu\right) > \frac{1}{4}[(1-p)\kappa_1 + p\kappa_2]^2 \quad \text{i.e. } \varepsilon < \varepsilon_p
$$

where

$$
\varepsilon_p = \frac{\sigma_1\sigma_2}{\sigma_1\nu + \frac{1}{4p(1-p)[(-p)\kappa_1 + p\kappa_2]^2}}.
$$

The maximum value of ε_p occurs at $p^* = \frac{\kappa_1}{\kappa_1 + \kappa_2}$ and is given by:

$$
\varepsilon^* = \frac{\sigma_1\sigma_2}{\sigma_1\nu + \kappa_1\kappa_2} \tag{A 14}
$$

Thus the two-time-scale original system is asymptotically stable for the singular perturbation parameter bound given in equation (A14).